NASA TECHNICAL NOTE

NASA TN D-2883

NASA TN D-2883

COMPARISONS OF EXPERIMENTAL HYDROXYL RADICAL PROFILES WITH KINETIC CALCULATIONS IN A SUPERSONIC NOZZLE

by Erwin A. Lezberg, Charles M. Rose, and Robert Friedman

Lewis Research Center
Cleveland, Ohio

NATIONAL AERONAUTICS AND SPACE ADMINISTRATION • WASHINGTON, D. C. • JUNE 1965

NASA TN D-2883

COMPARISONS OF EXPERIMENTAL HYDROXYL RADICAL PROFILES WITH KINETIC CALCULATIONS IN A SUPERSONIC NOZZLE

By Erwin A. Lezberg, Charles M. Rose, and Robert Friedman

Lewis Research Center
Cleveland, Ohio

NATIONAL AERONAUTICS AND SPACE ADMINISTRATION

For sale by the Clearinghouse for Federal Scientific and Technical Information
Springfield, Virginia 22151 – Price $2.00

COMPARISONS OF EXPERIMENTAL HYDROXYL RADICAL PROFILES WITH KINETIC CALCULATIONS IN A SUPERSONIC NOZZLE

by Erwin A. Lezberg, Charles M. Rose, and Robert Friedman

Lewis Research Center

SUMMARY

The hydroxyl (OH) mole fraction was determined from spectral line absorption measurements made in a supersonic nozzle that expanded the combustion products of hydrogen and preheated air. Absorption measurements were made as a function of fuel-air equivalence ratio (0.6 to 1.2) at combustor pressures of 3.6 and 1.8 atmospheres at low supersonic area ratios (1.6 to 3.55).

The measured OH mole fractions and previously reported static temperature measurements were compared to the output of a one-dimensional computer program that included finite rate chemistry. The conclusions drawn from these comparisons are as follows.

The controlling reaction is

$$H + OH + M \rightleftharpoons H_2O + M$$

Increasing or decreasing the rate of this reaction by a factor of three from the "standard rate" used in the calculations gives results compatible with the OH concentration measurements within the uncertainties involved in this measurement. Temperatures correlate best when a rate is used that is one-third the standard rate.

The recombination reaction

$$H + H + M \rightleftharpoons H_2 + M$$

becomes important only when its rate is comparable to or larger than the rate of the OH recombination reaction.

For lean mixtures a mechanism involving the reaction

$$H + O_2 + M \rightleftharpoons HO_2 + M$$

along with appropriate bimolecular HO_2 removal steps may be of importance since it offers an alternative recombination path.

INTRODUCTION

The calculation of nonequilibrium nozzle expansions has received a great deal of attention recently, and a number of computer programs have been written for calculating performance. Reaction rate data needed for input to these programs have generally been obtained from shock tube measurements or experiments using flat flame burners. Measurements of atom or radical recombination rates for the hydrogen-oxygen reactions have generally been inferred in shock tube experiments from the reverse dissociation rates at conditions far removed from equilibrium. The application of these rates to a nozzle expansion remains somewhat in question for critical comparisons since spread in recent data of at least an order of magnitude exists for the important three-body recombination reactions (refs. 1 to 3):

$$H + H + M \rightleftharpoons H_2 + M$$

$$OH + H + M \rightleftharpoons H_2O + M$$

(These are reactions (IV) and (V), respectively, as given in table I.)

The effects of third-body efficiency, particularly of water, are not well differentiated although some attempts at unravelling them in flat flame experiments have been made (ref. 3).

Some nozzle experiments have been reported in which measurements of static pressures (refs. 1 and 4) or temperatures (refs. 5 to 7) are compared with exact or approximate chemical kinetic calculations of performance. Reaction rates giving the best fit with the data have been inferred. In these comparisons, temperature measurements provide greater sensitivity to changes in rates than pressures. However, this does not allow separation of the effects of individual rates unless a single reaction such as (IV) or (V) is assumed to be controlling.

With the addition of a second measured variable, such as a species concentration that is reasonably sensitive to the rates, it should be possible to test the sensitivity of changes in the temperature and in the species concentration to changes in the rate constants. Hopefully, some improvement in knowledge of the appropriate rates could then be achieved by comparisons with the measurements.

The hydroxyl radical (OH) is known to be important to the kinetics of the hydrogen-oxygen reactions and is also spectroscopically accessible. Concentration of OH can be determined by spectral line absorption in the ultraviolet $^2\Sigma^+ \rightarrow {}^2\Pi$ electronic transition (ref. 8) by using known values for the transition probabilities.

The purpose of this investigation was to compare measurements of OH concentration and previously reported temperature measurements in a nozzle (ref. 5) with machine calculations by using an exact kinetic calculation. Calculations were also used in establishing the sensitivity of the calculated temperature and OH concentration to the various reactions.

Combustion products of hydrogen and preheated air were expanded through a supersonic nozzle. At a combustor pressure of 3.6 atmospheres, inlet air temperature was in the range 1710° to 1915° K. At a combustor pressure of 1.8 atmospheres, inlet air temperature was in the range 1725° to 1865° K. The range of equivalence ratios used was 0.6 to 1.2.

EXPERIMENTAL TECHNIQUES

Facility and Instrumentation

A description of the experimental facility and basic instrumentation is given in reference 9. Combustor inlet conditions for a Mach 6, subsonic-burning ramjet were simulated by using an alumina pebble bed to supply air at temperatures up to 1900° K and pressures up to 3.6 atmospheres to a water-cooled combustion chamber and nozzle.

Hydrogen fuel was supplied from a cylinder trailer. It was injected into the combustion chamber through water-cooled fuel injection tubes drilled with 148 orifices 0.040 inch in diameter. The orifices were arranged to cover approximately equal areas of the combustor cross section. A DeLaval nozzle with a 3.2-inch-diameter throat and a 7° half-angle divergent cone was equipped with 1/2-inch-diameter optical ports downstream of the nozzle throat. The ports were purged with air during a run to keep the quartz windows clean. Static-pressure taps were drilled normal to the nozzle wall, and wall thermocouples were mounted flush with the inside wall.

Hydroxyl Absorption Measurements

The concentration of the OH radical was determined by line absorption in the ultraviolet $^2\Sigma^+ - {}^2\Pi$ electronic band (ref. 8). The description of the apparatus and method is given in some detail in reference 10. The apparatus is shown schematically in figure 1. The light source is an end-view capillary discharge tube that is operated with a water vapor pressure of about 1.0 millimeter of mercury. The emission line of the cooled source is absorbed by the broader absorption line of the combustion gases so that ideally only absorption at the line center is measured.

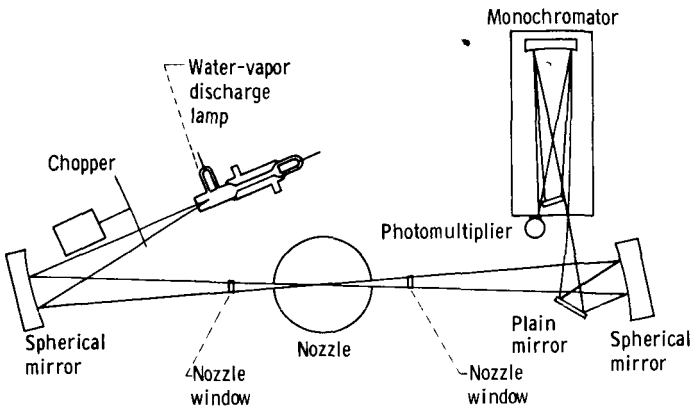

Figure 1. - Optical arrangement for line absorption measurements.

Procedure and Data Reduction

Transmission measurements were made in the O-O vibrational band by using Q branch rotational lines from K = 12 to 19. This selection of rotational lines was made so that the absorption followed the Beers' Law Relation.

The absorption measurements were made by first scanning past a spectral line of the lamp with a nonabsorbing gas (air) flowing through the nozzle and then by scanning the same line with the absorbing gas (hydrogen-air combustion products) in the light path. Since the light was chopped on the source side, and only the chopped signal was amplified, possible emission from the gas was not recorded.

The absorption at the line center is related to the ground electronic-state population by the f numbers for the transition and the shape of the absorption line. The f number is defined as the ratio of the number of dispersion electrons to the number of absorbers and is related to the electronic transition probability. (All symbols are defined in appendix A.)

The concentration of OH in the ground state is given by (ref. 10)

$$N_{OH} = \frac{Q_{R,V} b_D P'}{F A_K T_{J'J''}} \exp\left(\frac{hc\omega_K}{kT}\right) \times 2.40 \times 10^{12} \tag{1}$$

where $Q_{R,V}$ is the rotation-vibration partition function, b_D the Doppler half-width of the absorption line, and $A_K T_{J'J''}$ the relative transition probabilities including the effects of vibration-rotation interaction (ref. 11).

The exponential term, which is the Boltzmann factor for the rotational distribution, was evaluated at the measured sodium spectral line (ref. 9) reversal temperature. The value of F, where

$$F = f \frac{2J'' + 1}{A_K}$$

is taken as $2.0 \times 10^{-4} \pm 10$ to 15 percent (refs. 12 and 13). The absorption coefficient P' is determined as the natural log of the measured reciprocal transmittance I_0/I, where I_0 is the source intensity and I is the source intensity attenuated by the absorbing gas.

The calculation of N_{OH} from equation (1) is exact when assuming an infinitely narrow source width and pure Doppler broadening of the absorber line. Corrections for an assumed finite width of emission line and a combination of Doppler and collision broadening of absorber line can be made by replacing P' in equation (1) with the equivalent absorption coefficient at the center of a Doppler broadened line where the integral of the absorption coefficient over the Doppler line is equal to the integral for the actual line shape:

$$\int_D P'_\omega \, d\omega = \int_{line} P_\omega \, d\omega \tag{2}$$

The corrections are discussed in appendix B. The total correction increased the value of the absorption coefficient by about 20 percent at a chamber pressure of 3.6 atmospheres and 17 percent at a pressure of 1.8 atmospheres.

Sources of Error

Checks of rotational equilibrium were made by scanning a portion of the spectrum and determining the absorption coefficient

$$P_{\omega_o} = \ln \frac{I_0}{I}$$

for a number of lines in the O-O band. The rotational temperature can be determined by plotting $\log P_{\omega_o} / A_K T_{J'J''}$ against the rotational energy of the transition and by taking the slope of the resulting straight line. Within experimental error, the lines were straight and the temperature was generally within 100° K of the sodium reversal temperature measured at the nozzle centerline (ref. 9). The determination of the rotational temperature involved absorption measurements of some stronger lines that were 90 percent or more absorbed and, therefore, subject to errors because of self-absorption. Changes in I_0 could occur through slight dirtying of the test section windows, through changes in source current or pressure, or through the movement of the source image with respect to the entrance slit due to vibration or refraction of the light by density gradients in the test gas. The change in the source intensity from these effects was usually less than 5 percent. The low-frequency noise level of the source was about 3 percent. Errors in the sodium reversal-temperature measurement could result in concentration errors due to the temperature effect on the population distribution, the half-width, and the gas density. A 5-percent error in the reversal temperature would result in a 4-percent error in the OH mole fraction for the $Q_1 15$ line at 1850° K.

Additional errors are introduced in the calculation of OH mole fraction by the uncertainty in the F value (10 to 15 percent) and in the corrections for the line shape and width (≈20 percent).

CALCULATIONS

Description of Nozzle Kinetic Program

An IBM 7094 computer program for the solution of the one-dimensional flow of reacting gases in a nozzle is described in references 15 and 16. Input information is in the form of tables of specific heat data, equilibrium constant data, nozzle area coordinates, and reaction rate data for a set of up to 15 reactions. The minimum number of reactions is equal to the total number of species minus the number of atom species. Starting conditions are initial values of pressure, temperature, velocity, and species concentrations.

The program can be started at equilibrium or nonequilibrium conditions, and it will accept starting conditions either in the subsonic or supersonic portion of the nozzle. The problem of the singularity at the sonic point is handled by transforming the equation system in the transonic region to allow Mach number to be the independent variable rather than area. This results in slight alterations of the throat contour.

Starting conditions for the kinetic program were computed from an equilibrium program (ref. 14). The equilibrium program computed combustor and nozzle conditions by starting with measured values of combustion air and fuel temperatures, pressure, and fuel-air ratio. The calculated equilibrium combustion temperature was not corrected for cooling losses to the combustion chamber and nozzle. Previous combustion temperature measurements (ref. 9) indicated that measured core temperatures were not affected by the cooled walls. Generally, starting conditions were taken from the equilibrium calculations at subsonic area ratios of 1.54 or 1.04. In some cases where the expansion remained closer to equilibrium, the kinetic program was started downstream of the throat at an area ratio of 1.01 to save computing time.

Assumed Reaction Mechanism and Rate Constants

Table I lists the standard set of reactions and rate constants used for comparison with the experimental results. The rates used for the hydrogen atom recombination reactions (IV) and (V) were taken from reference 5 since they had shown good agreement with experimental temperature measurements when compared with the Bray freezing point

TABLE I. - RATES OF REACTIONS USED WITH KINETIC PROGRAM

[Units are cu cm, g mole, sec, and ^{o}K.]

Reaction	Standard rate	Reference
(I) $H_2 + OH \rightleftharpoons H + H_2O$	$^{a}k_I = (4.2\times10^{12})T^{1/2}e^{-10000/RT}$	27
(II) $H + O_2 \rightleftharpoons O + OH$	$k_{II} = (5.64\times10^{13})e^{-15100/RT}$	27
(III) $O + H_2 \rightleftharpoons H + OH$	$k_{III} = (1.2\times10^{13})e^{-9200/RT}$	27
(IV) $H + H + M \rightleftharpoons H_2 + M$	$^{b}k_{IV} = (3.0\times10^{18})T^{-1}$	5
(V) $OH + H + M \rightleftharpoons H_2O + M$	$^{a}k_V = (7.5\times10^{19})T^{-1}$	5
(VI) $O + O + M \rightleftharpoons O_2 + M$	$k_{VI} = (1.85\times10^{17})T^{-1/2}$	27
(VII) $NO + M \rightleftharpoons N + O + M$	$k_{VII} = (1.06\times10^{25})T^{-2.5}e^{-154000/RT}$	27
(VIII) $O + N_2 \rightleftharpoons N + NO$	$k_{VIII} = (1.01\times10^{12})T^{1/2}e^{-75500/RT}$	27
(IX) $N + O_2 \rightleftharpoons O + NO$	$k_{IX} = (1.02\times10^{11})T^{1/2}e^{-6200/RT}$	27

[a]Rate variations were times 1/3 and 3.

[b]Rate variations were times 1/10 and 100.

analysis. Variations in the rates of reactions (I), (IV), and (V) were assumed to have the greatest effect on the overall kinetics (refs. 17 and 18).

RESULTS AND DISCUSSION

Hydroxyl Concentrations

The experimental OH mole fractions, calculated by using equation (1), are given as a function of fuel-air equivalence ratio at nozzle supersonic area ratios of 1.6, 2.02, 2.49, and 3.55 in figures 2(a) and (b). The stagnation pressures are 3.6 and 1.8 atmospheres, respectively. A dashed line was faired through the data for the $Q_1 15$ line.

Discrepancies in the experimental data obtained at the higher area ratios were observed when different rotational lines were used in the transmission measurements. The higher energy lines (e.g., $Q_1 15$) yielded the higher values of mole fraction. The differences might be attributed to a combination of radial temperature profile and self-absorption, although an attempt at resolving the differences by assuming a temperature profile was not successful.

The lower lines on figures 2(a) and (b) were calculated for equilibrium flow by using the IBM 7094 program of reference 14. Comparisons of the data with these equilibrium calculations indicate at least partial freezing of the OH mole fraction. It can be noted that the data show no significant effect of pressure and a much smaller dependence on equivalence ratio than the equilibrium curves.

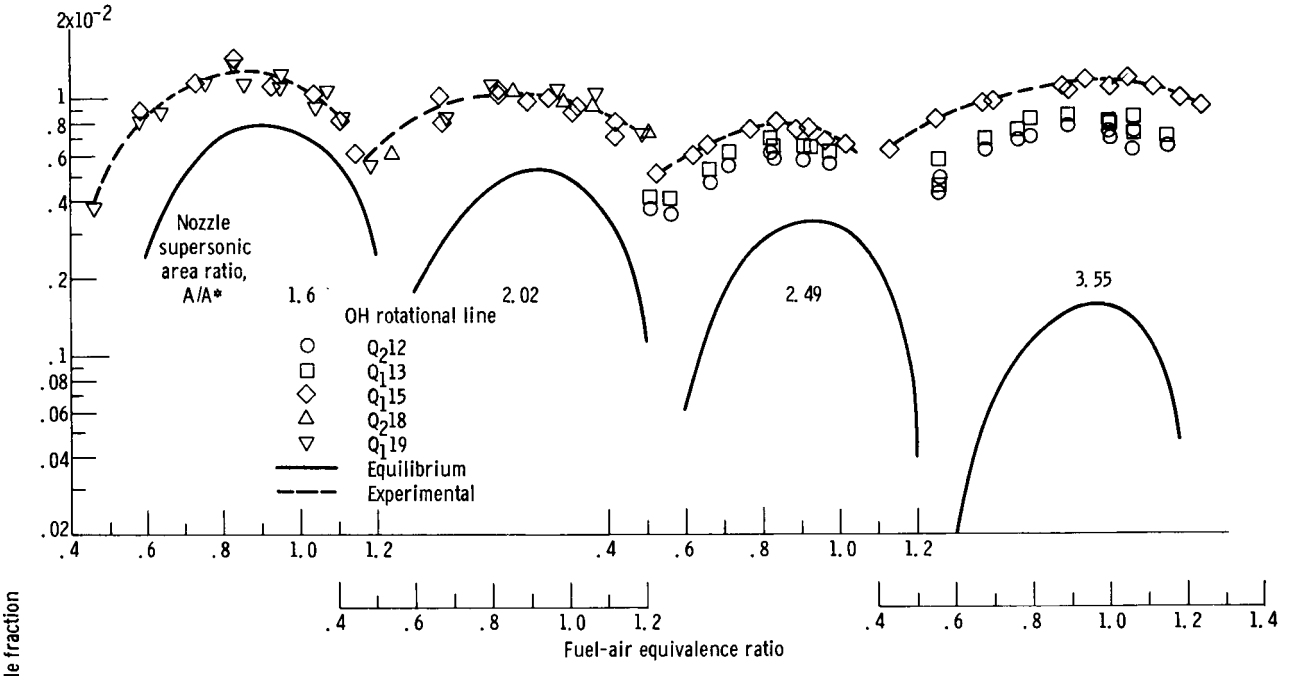

(a) Initial pressure, 3.6 atmospheres; air temperature, 1710° to 1915° K.

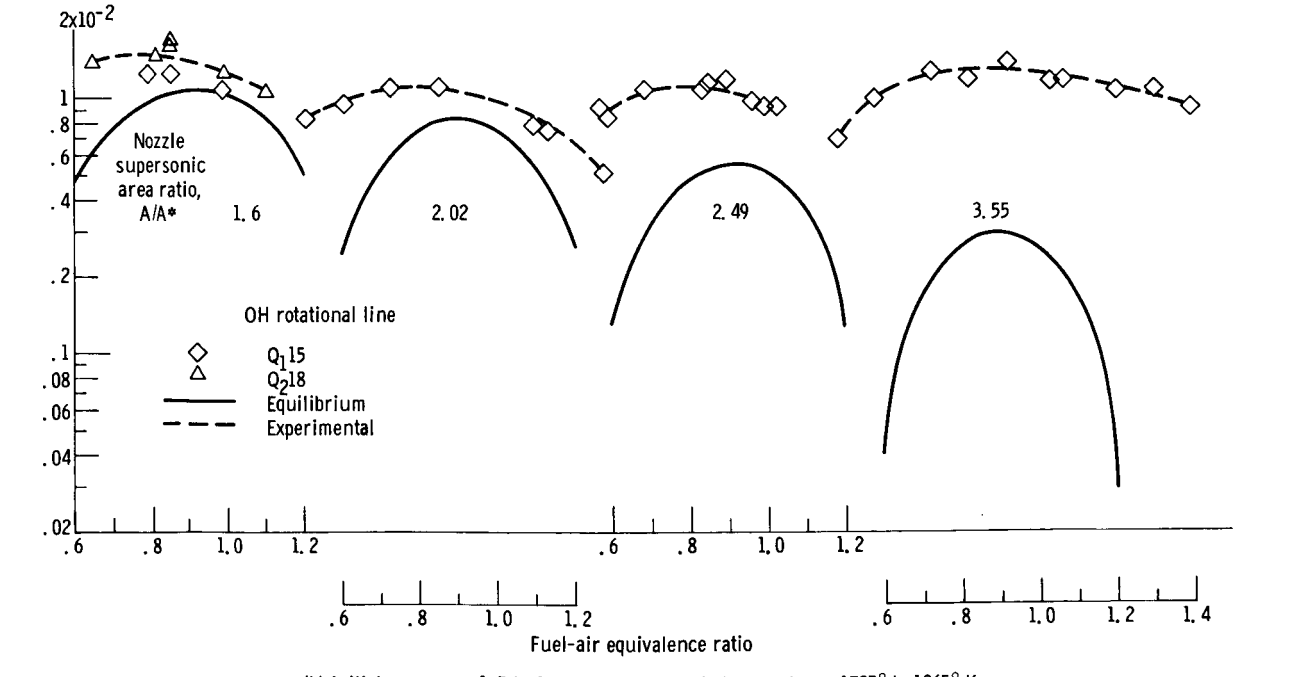

(b) Initial pressure, 1.7 to 1.9 atmospheres; air temperature, 1725° to 1865° K.

Figure 2. - Hydroxyl concentration by line absorption of $^2\Sigma^+ \rightarrow {}^2\Pi$ transition; 0-0 vibrational band. Hydrogen-air combustion products.

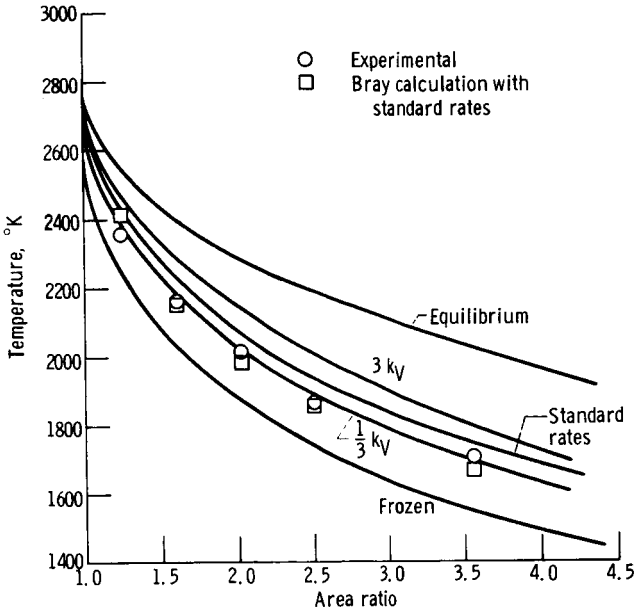

Figure 3. - Comparison of measured and calculated static temperatures. Variation of rate constant for $H + OH + M \rightleftarrows H_2O + M$; chamber pressure, 3.6 atmospheres; equivalence ratio, 1.0.

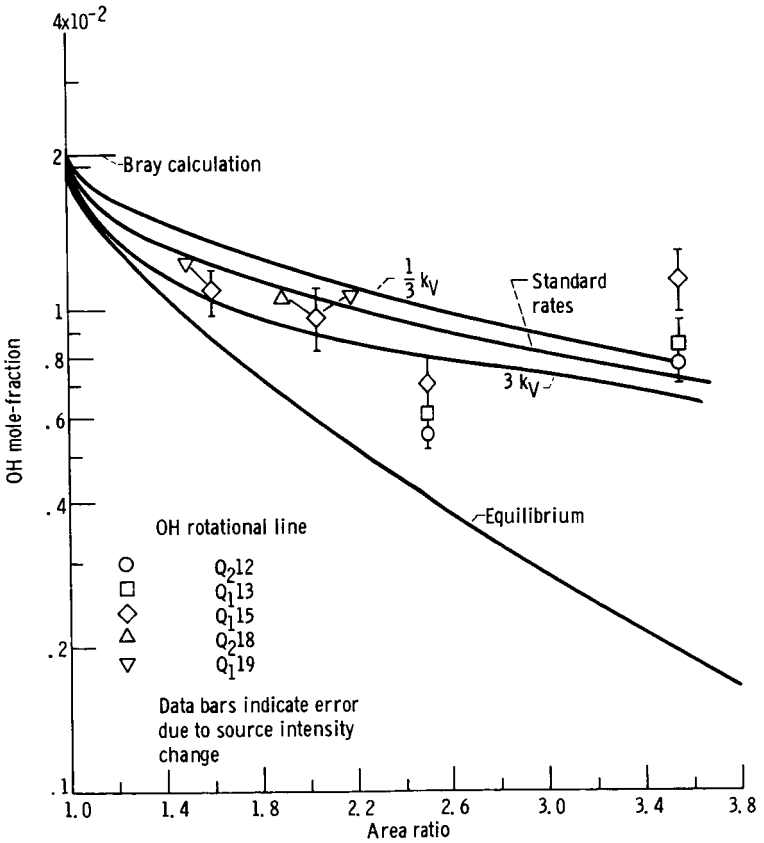

Figure 4. - Comparison of measured and calculated OH mole fraction. Variation of rate constant for $H + OH + M \rightleftarrows H_2O + M$; chamber pressure, 3.6 atmospheres; equivalence ratio, 1.0.

Comparisons with Kinetic Nozzle Calculations

The experimental data are compared at a combustor pressure of 3.6 atmospheres and at the stoichiometric fuel-air ratio with the kinetic calculations by using the standard rates and variations of the rate of reaction (V) (figs. 3 and 4).

Figure 3 compares measured reversal temperatures along the axis of the nozzle (ref. 5) with temperatures calculated with the kinetic program by using variations of one-third, one, and three times the standard rate in reaction (V). The limiting cases of equilibrium and frozen flow and the calculations performed with the Bray freezing analysis are also indicated. The measured temperatures are seen to be about 70° K below the calculations that used the standard rates. A better comparison is indicated by k_V times one-third. The Bray calculations that use the standard recombination rates compare quite well with the data, but they yield conservative values when compared to the complete kinetic calculation.

Figure 4 compares the measured OH mole fraction with kinetic calculations. The data bars indicate the uncertainty in the measurement due to source intensity changes. If the differences introduced by using different rotational lines at the higher area ratios and the probable error in the f value and line shape corrections are considered, the measured OH mole fractions are consistent with the calculations that use values of k_V between one-third and three times the standard rate.

Figures 5 and 6 show comparisons of the data at 3.6 atmospheres and at an equivalence ratio of 0.6 with the kinetic calculations using the standard rates. The measured temperatures and OH mole fractions are in slightly better agreement than the data taken at $\varphi = 1.0$.

Comparisons of the data with calculations at a combustor pressure of 1.8 atmospheres and at the stoichiometric fuel-air ratio are shown in figures 7 and 8. The measured temperatures and Bray calculations are about 50° K below the kinetic calculations. Measured OH mole fractions are in only fair agreement with the calculations.

Sensitivity of Calculations to Changes in Rate Constants

The proximity of a reaction to equilibrium can be inferred by the parameter λ when

$$\lambda_j = K_{EQ_j} \prod_i C_i^{(\nu' - \nu'')_{ij}} \tag{3}$$

where C_i is the concentration of specie i and ν' and ν'' are the stoichiometric coefficients of reactants and products, respectively (in reaction j). The parameter λ_j

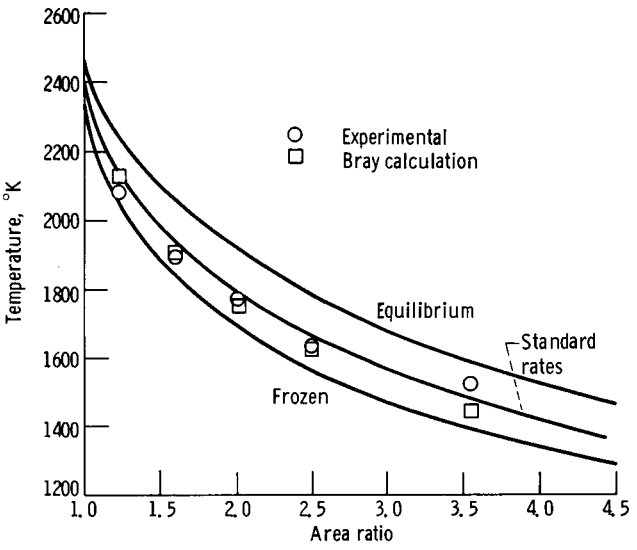

Figure 5. - Comparison of measured and calculated static temperatures. Standard reaction rates; chamber pressure, 3.6 atmospheres; equivalence ratio, 0.6.

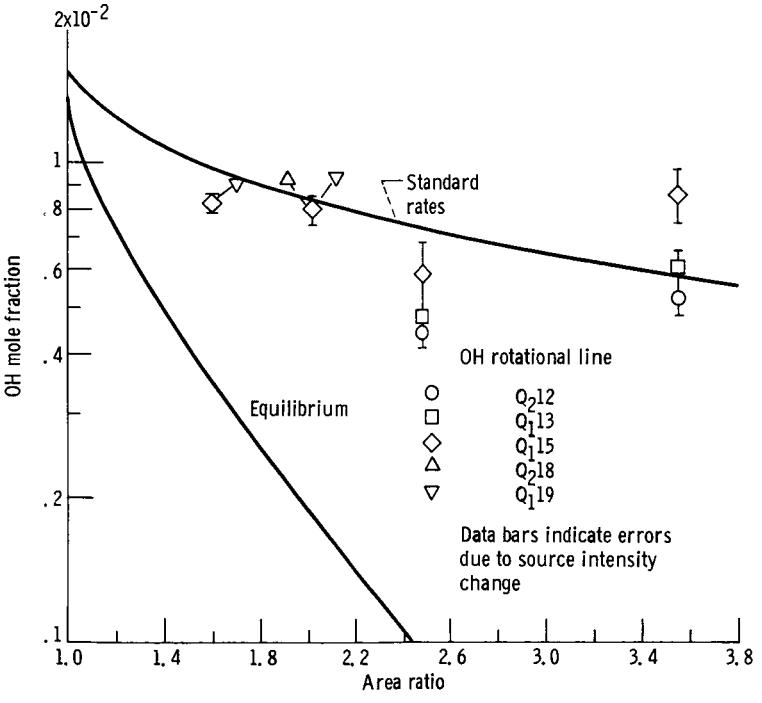

Figure 6. - Comparison of measured and calculated OH mole fraction. Standard reaction rates; chamber pressure, 3.6 atmospheres; equivalence ratio, 0.6.

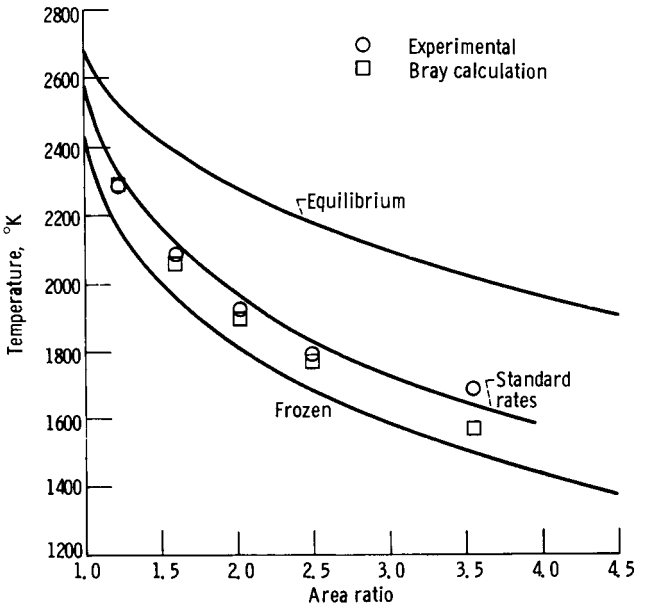

Figure 7. - Comparison of measured and calculated static temperatures. Standard reaction rates; chamber pressure, 1.8 atmospheres; equivalence ratio, 1.0.

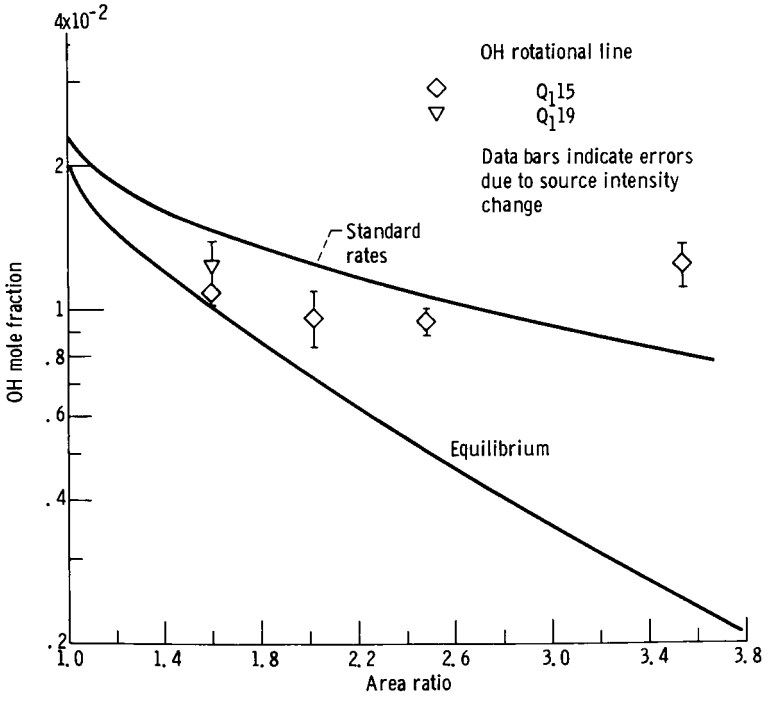

Figure 8. - Comparison of measured and calculated OH mole fraction. Chamber pressure, 1.8 atmospheres; equivalence ratio, 1.0.

TABLE II. - DEPARTURE FROM EQUILIBRIUM FOR VARIOUS REACTIONS WHEN STANDARD REACTION RATES ARE USED

Area ratio	Lambda parameter[a] for first five reactions				
	λ_I	λ_{II}	λ_{III}	λ_{IV}	λ_V
1.00	1.00029	1.00837	1.02008	1.27743	1.39532
1.46	1.00142	1.01209	1.03396	14.7317	17.8923
1.95	1.00268	.99934	1.01522	102.259	130.555
2.66	1.00590	.98234	.99445	1 015.50	1 388.24
3.19	1.00935	.97165	.98513	4 382.15	6 269.06
4.16	1.01917	.95512	.98053	42 336.7	65 282.0

[a]For the j^{th} reaction, $\lambda_j = K_{EQ_j} \prod_i C_i^{(\nu' - \nu'')_{ij}}$.

is evaluated by the kinetic program and is listed in table II for the first five reactions as a function of area ratio. Because of the definition of the equilibrium constant, $\lambda = 1$ at equilibrium. It is noted that reactions (I) to (III) remain near equilibrium throughout the area ratio range shown, whereas reactions (IV) and (V) depart from equilibrium upstream of the throat.

Kinetic calculations were made to determine the effect of changing the rate constants of reactions (I) and (IV) (see table I, p. 7). The calculations for temperature and OH mole fraction are shown in figures 9 and 10. No significant difference in temperature or OH mole fraction is introduced by changing the rate of the bimolecular reaction (I) by factors of one-third or three times the standard rate. This range is somewhat wider than the range of rate constants for reaction (I) found in the literature. The insensitivity to bimolecular rates was expected in view of the assumption (ref. 18) that the bimolecular reactions are in equilibrium with each other for the hydrogen-oxygen system.

A decrease in the rate of the hydrogen atom recombination reaction by a factor of 10 showed no significant change in the variables calculated by using the standard rates. An increase in this rate by a factor of 100, however, clearly allows this reaction to be controlling, and the calculated temperatures and mole fractions are shifted closer to equilibrium. Since the standard rate constant for reaction (V) was a factor of 25 greater than that of reaction (IV), it is anticipated that significant effects would be noted if the rate of reaction (IV) were about equal or greater than reaction (V).

Sensitivity of Calculations to Changes in Reaction Mechanism

Fenimore and Jones (ref. 19) have inferred from some measurements in lean

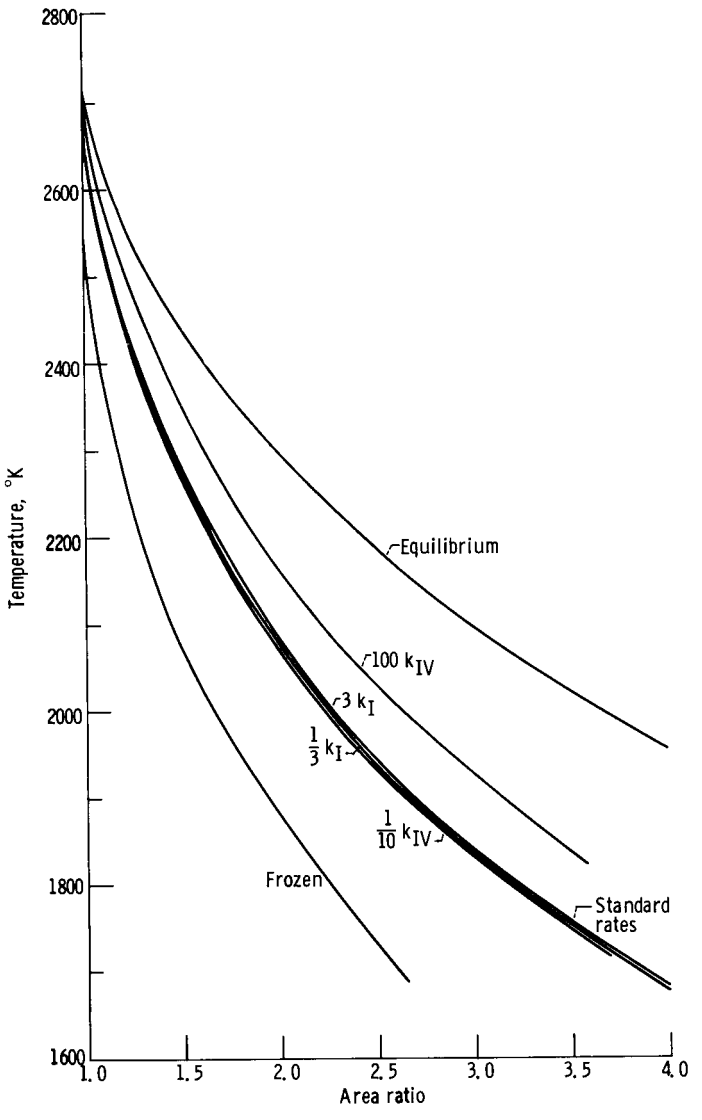

Figure 9. - Effects of variation of rate constant data on static temperature. Chamber pressure, 3.6 atmospheres; equivalence ratio, 1.0.

hydrogen-oxygen-argon flames that a recombination reaction involving HO_2 may be important. The reaction scheme proposed is the three-body recombination reaction

$$H + O_2 + M \rightleftharpoons HO_2 + M \qquad \Delta H = -47 \text{ kcal} \qquad \text{(X)}$$

followed by the removal steps

$$HO_2 + H \rightarrow 2\ OH \qquad \Delta H = -38 \text{ kcal} \qquad \text{(XI)}$$

$$HO_2 + OH \rightarrow O_2 + H_2O \qquad \Delta H = -38 \text{ kcal} \qquad \text{(XII)}$$

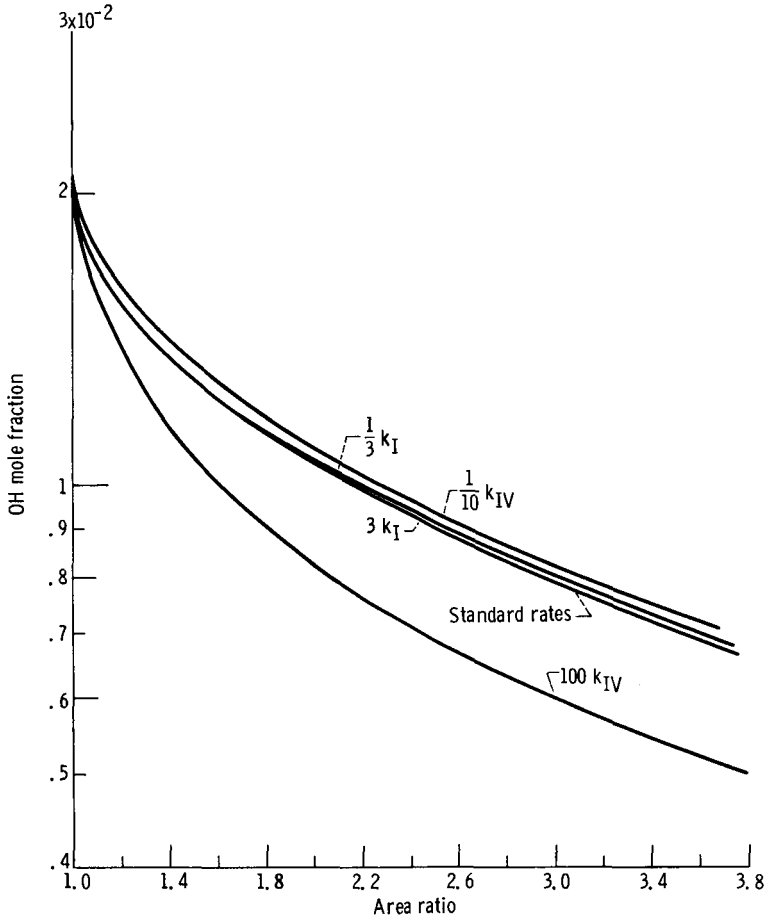

Figure 10. - Effects of variation of rate constant data on OH mole fraction. Chamber pressure, 3.6 atmospheres; equivalence ratio, 1.0.

A rate for reaction (X) was inferred from low temperature data (refs. 19 to 21), an assumed T^{-1} temperature dependence, and weighted third-body efficiencies (rate calculated by Frank Belles, Lewis Research Center). The rate constant is given as

$$k_X = 7.25 \times 10^{19} T^{-1} \quad (cm^6)(mole^{-2})(sec^{-1})$$

The rate constants for reactions (XI) and (XII) were assumed to be

$$k_{XI,\,XII} = 10^{14} e^{-5000/RT} \quad (cm^3)(mole^{-1})(sec^{-1})$$

Since the rate given in reference 19 is comparable with reaction (V), it would be likely to be of some importance at least in lean flames.

Kinetic calculations were performed at equivalence ratios of 0.6 and 1.0 with the addition of reactions (X) to (XII) to the reaction scheme. The rates used were taken from table I (p. 7) with k_V times one and times one-third. The reduction in k_V was used to

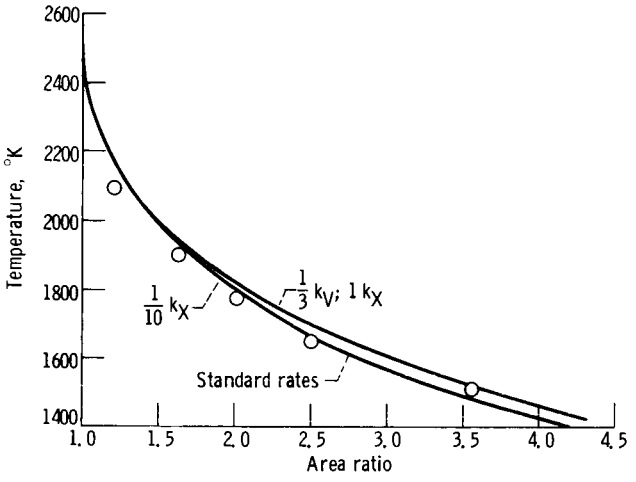

Figure 11. - Comparison of measured and calculated temperatures for a change in reaction mechanism; variation of rate constants for reactions V ($H + OH + M \rightleftarrows H_2O + M$) and X to XII ($H + O_2 + M \rightleftarrows HO_2 + M$, $HO_2 + H \rightleftarrows 2\,OH$, and $HO_2 + OH \rightleftarrows O_2 + H_2O$); chamber pressure, 3.6 atmospheres; equivalence ratio, 0.6.

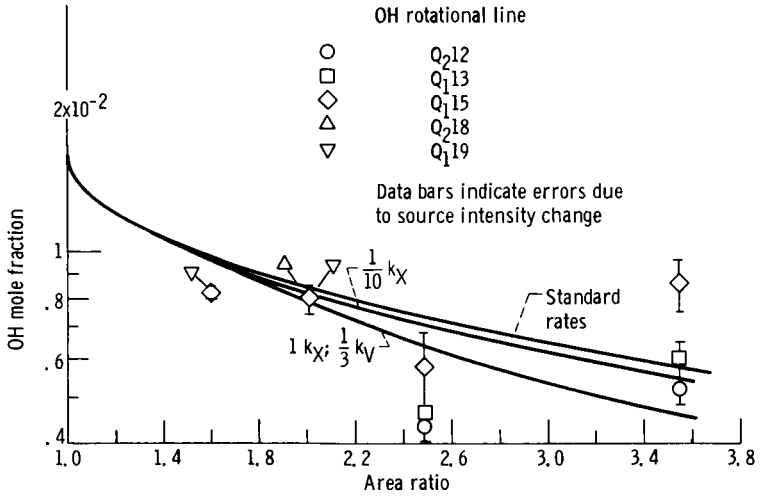

Figure 12. - Comparison of measured and calculated OH mole fraction for a change in reaction mechanism; variation of rate constant for reactions V ($H + OH + M \rightleftarrows H_2O + M$) and X to XII ($H + O_2 + M \rightleftarrows HO_2 + M$, $HO_2 + H \rightleftarrows 2\,OH$, and $HO_2 + OH \rightleftarrows O_2 + H_2O$); chamber pressure, 3.6 atmospheres; equivalence ratio, 0.6.

counter the effect on temperature of the additional recombination path since values of k_V obtained from the literature would have included effects of k_X if it has been important in the reaction scheme.

The results of the calculations that used the alternate reaction mechanism are shown compared with the standard rates and the experimental data in figures 11 and 12 for an equivalence ratio equal to 0.6 and $p_c = 3.6$ atmospheres. Results at an equivalence ratio of 1.0 and using k_V times one showed negligible differences from the standard set of reactions because of the low oxygen concentration.

At an equivalence ratio of 0.6, the effect of including reactions (X) to (XII) more than compensated for the decrease in k_V. Since the rates of reactions (X) to (XII) are uncertain, a further comparison was made with the standard set of rate constants and k_X times one-tenth. The temperatures were not significantly different with or without reaction (X), but the OH mole fraction (fig. 12) showed a slight decrease. It appears that calculations which use some other combination of k_V and k_X might compare more favorably with the data at an equivalence ratio of 0.6, but the uncertainties in the experimental data would not justify any conclusions as to their relative magnitudes. Further experimental determinations of the rates of reactions (V) and (X) to (XII) are needed for clarification of the recombination kinetics for lean mixtures.

SUMMARY OF RESULTS

Hydroxyl (OH) mole fractions were determined from spectral line absorption measurements in a supersonic nozzle expanding the combustion products of hydrogen and preheated air. Measurements were made as a function of fuel-air equivalence ratio (0.6 to 1.2) at combustor pressures of 3.6 and 1.8 atmospheres at low supersonic area ratios (1.6 to 3.55).

The measured OH mole fractions and previously reported static temperature measurements were compared to values of these parameters calculated by a one-dimensional computer program which included finite rate chemistry. The conclusions drawn from these comparisons are as follows:

1. The OH radical concentration and temperature measurements compare reasonably well with the kinetic computations that use a standard set of rate constants. The results of the OH concentration measurements are compatible with a rate constant for the reaction

$$H + OH + M \rightleftharpoons H_2O + M$$

within a factor of three higher or lower than the standard rate. The temperature measurements indicate a rate for the preceding reaction somewhat less than the standard rate.

2. The insensitivity of the temperature and concentration to the bimolecular rates indicates that the partial equilibrium hypothesis is acceptable for the range of conditions investigated.

3. Changes in OH mole fraction and temperature are sensitive to the recombination reactions

$$H + H + M \rightleftharpoons H_2 + M$$

$$H + OH + M \rightleftharpoons H_2O + M$$

The hydrogen recombination reaction only becomes important when its rate is comparable to or larger than the rate of the water recombination reaction.

4. For lean mixtures, the recombination reaction

$$H + O_2 + M \rightleftharpoons HO_2 + M$$

followed by the removal steps

$$HO_2 + H \rightarrow 2OH$$

$$HO_2 + OH \rightarrow O_2 + H_2O$$

may be of importance since it offers an alternative recombination path.

Lewis Research Center,
National Aeronautics and Space Administration,
Cleveland, Ohio, April 2, 1965.

APPENDIX A

SYMBOLS

A/A^*	nozzle supersonic area ratio
A_K	relative line strength
A_α	absorptance
a	broadening parameter
b	half width at half intensity, cm^{-1}
C	concentration, moles/cu cm
c	speed of light, cm/sec
F	$f(2J'' + 1)/A_K$, function
f	ratio of number of dispersion electrons to number of absorbers
h	Planck constant
I	relative intensity
J	rotational quantum number
K	$J \pm \frac{1}{2}$
K_{EQ}	equilibrium constant
k_j	rate constant, j = I, II · · · XII
k	Boltzmann constant
ℓ	path length, cm
m	atomic mass
N	number density, cm^{-3}
P	absorption coefficient
P'	absorption coefficient for a Doppler shaped line
p	pressure, atm
$Q_{R,V}$	rotational-vibrational partition function
R	gas constant
T	temperature, ^oK
$T_{J'J''}$	correction factor to line strengths for vibration-rotation interaction
y	variable of integration
α	ratio of source line to absorber line widths
λ	defined by eq. (3)
ν	stoichiometric coefficient
φ	fuel-air equivalence ratio
ω	wave number, cm^{-1}

Subscripts:

A	absorption line
C	collision
c	chamber
D	Doppler
E	emission line
i	species
j	reaction
K	rotational line designation
N	natural
ω	wave number
ω_o	wave number at line center
0	initial

Superscripts:

'	reactant
''	products

APPENDIX B

EVALUATION OF LINE SHAPE CORRECTIONS

Equation (1) (p. 4) is exact when P' represents the absorption coefficient at the center of a Doppler shaped line. Since the OH absorption lines are partially collision broadened and the source emission lines have finite width, corrections must be made to the absorption coefficient in equation (1) so that the integral over the absorption line represents the value for the actual line shape.

The absorptance is related to the absorption coefficient at the line center by (ref. 22, pp. 122 and 169)

$$A_\alpha = \frac{I_0 - I}{I_0} = \frac{\int_{-\infty}^{\infty} \exp\left(-\frac{\omega_1^2}{\alpha^2}\right)\left\{1 - \exp\left[-P'\ell\left(\frac{P_\omega}{P'}\right)\right]\right\}d\omega}{\int_{-\infty}^{\infty} \exp\left(-\frac{\omega_1^2}{\alpha^2}\right)d\omega} \tag{B1}$$

where

$$\omega_1 = \frac{\omega - \omega_o}{\Delta\omega_A} 2\sqrt{\ln 2} \tag{B2}$$

and

$$\alpha = \frac{\Delta\omega_E}{\Delta\omega_A} = \frac{b_{D(E)}}{\left(b_C + b_D\right)_A} \tag{B3}$$

with b_D and b_C as the Doppler and collision half widths at half intensity.

The collision half width of the absorption line can be written in terms of the broadening parameter a where

$$a = \frac{b_N + b_C}{b_D} (\ln 2)^{1/2} \tag{B4}$$

When the natural half width b_N is neglected in comparison with b_C, equation (B3) becomes

$$\alpha = \frac{b_{D(E)}}{b_{D(A)}} \frac{1}{1 + a(\ln 2)^{-1/2}} \tag{B5}$$

For optically thin emission and absorption lines, the ratio of Doppler half widths is equal to the square root of the absolute temperature ratio and

$$\alpha = \sqrt{\frac{T_E}{T_A}} \frac{1}{1 + a(\ln 2)^{-1/2}} \tag{B6}$$

Equation (B1) has been evaluated for Doppler shaped absorption lines in appendix IV of reference 22, where the absorption term is $1 - \exp\left[-P'\ell \exp\left(-\omega_1^2\right)\right]$.

It can also be evaluated from the series expansion

$$A_\alpha = \frac{P'\ell}{\left(1 + \alpha^2\right)^{1/2}} - \frac{(P'\ell)^2}{2!\left(1 + 2\alpha^2\right)^{1/2}} + \cdots + (-1)^n \frac{(P'\ell)^n}{n!\left(1 + n\alpha^2\right)^{1/2}} \tag{B7}$$

For combined Doppler and collision broadening, the absorption coefficient is related to the coefficient at the line center by (ref. 22)

$$\frac{P_\omega}{P'} = \frac{a}{\pi} \int_{-\infty}^{\infty} \left[a^2 + (\omega - y)^2\right]^{-1} \left[\exp(-y^2)\right] dy \tag{B8}$$

where

$$P' = \frac{\int_{-\infty}^{\infty} P_\omega \, d\omega}{\omega_o} \left(\frac{mc^2}{2\pi k T}\right)^{1/2} \tag{B9}$$

is the absorption coefficient at the center of a Doppler broadened line.

For small values of a equation (B8) can be written as an expansion around the Doppler contour (ref. 23):

$$\frac{P_\omega}{P'} = \exp\left(-\omega_1^2\right) - 2a^{-1/2}\left[1 - 2\omega_1 F(\omega_1)\right] + a^2\left(1 - 2\omega_1^2\right)\exp\left(-\omega_1^2\right)$$

$$-2a^3 - \frac{1}{2}\left[\frac{2}{3}\left(1 - \omega_1^2\right) - 2\omega_1\left(1 - \frac{2}{3}\omega_1^2\right)F(\omega_1)\right] + \cdots \tag{B10}$$

In order to determine the proper value of P' to use in equation (1), an approximate approach was used here in which the corrections for finite emitter line width and absorber line shape were evaluated separately. As a first approximation, the absorption line was assumed to be Doppler broadened only, and the right side of equation (B1) evaluated from the approximate relation (B7) and the tabular values of appendix IV in reference 22. Values of $P_{\omega_o} \ell$ were plotted as functions of

$$\frac{I_0}{I} = \frac{1}{1 - A_\alpha}$$

for various values of α. The value of the absorption coefficient is obtained from the plot by using experimental values of I_0/I, α, and the path length ℓ. Equation (B10) is evaluated at the line center where $\omega_1 = 0$ and where P_{ω_o}/P', the ratio of the absorption coefficient for the actual line shape to the coefficient for a Doppler shaped line, is obtained. When the values determined for P_{ω_o} and P_{ω_o}/P' are used, the appropriate value for P' can then be substituted in equation (1). The total correction increased the value of the absorption coefficient by about 20 percent at a chamber pressure of 3.6 atmospheres and 17 percent at a pressure of 1.8 atmospheres.

The error in using the Doppler form of equation (B1) was evaluated for the experimental data having the largest values of the broadening parameter a by numerical integration using equations (B1) and (B10). The approximate correction was found to yield values of the absorption coefficient which were a maximum of 10 percent low, and most of the data had errors in the absorption coefficient which were well under this value. In view of much larger uncertainties in the parameters a and α, use of the more exact expression was not justified.

The broadening parameter a was evaluated from (ref. 24)

$$a = 335 \frac{p}{T} \tag{B11}$$

and from measured values of the static pressure and temperature. Equation (B11) is an empirical relation derived from the pressure and temperature dependence of the collision and Doppler widths.

Carrington (ref. 25) has evaluated the parameter a by using the curve of growth and has reported $a = 0.05 \pm 0.05$. At the temperature of his flame,[1] equation (B11) gives a value of $a = 0.117$. Kaskan (ref. 26) has given $a = 450 \frac{p}{T}$ as best fitting his experi-

[1]Carringtons' measured rotational temperature of 2660° K has been corrected to 2866° K by Learner (ref. 11) for vibration-rotation interaction.

mental measurements at temperatures around 1500° K. Considering the uncertainty in the values of references 25 and 26, equation (B11) is consistent with either.

The value of α is calculated from equation (B6) by using the measured reversal temperatures for T_A and a source translational temperature taken somewhat arbitrarily as $T_E = 500^{\circ}$ K. The source rotational distribution could not be characterized by a single temperature, but the distribution curve appeared to have an asymptotic slope for rotational quantum numbers less than or equal to $K = 3$, which gave the above value. A value of $T_E = 450^{\circ}$ K has been reported for a similar discharge source (ref. 13).

REFERENCES

1. Russo, A. L.; Hall, J. G.; and Lordi, J. A.: Experimental Studies of Chemical Nonequilibrium in Hydrogen Nozzle Flows. Rept. No. CAL-AD-1689-A-4, Cornell Aero. Lab., June 1964.

2. Bulewicz, E. M.; and Sugden, T. M.: The Recombination of Hydrogen Atoms and Hydroxyl Radicals in Hydrogen Flame Gases. Trans. Faraday Soc., vol. 54, 1958, pp. 1855-1860.

3. Rosenfeld, J. L. J.; and Sugden, T. M.: Burning Velocity and Free Radical Recombination Rates in Low Temperature Hydrogen Flames. II - Rate Constants for Recombination Reactions. Combustion and Flame, vol. 8, no. 1, Mar. 1964, pp. 44-50.

4. Widawsky, Arthur; Oswalt, Lawrence R.; and Harp, James L., Jr.: Experimental Determination of the Hydrogen Recombination Constant. ARS J., vol. 32, no. 12, Dec. 1962, pp. 1927-1929.

5. Lezberg, Erwin A.; and Franciscus, Leo C.: Effects of Exhaust Nozzle Recombination of Hypersonic Ramjet Performance. AIAA J., vol. 1, no. 9, Sept. 1963, pp. 2071-2083.

6. Hoglund, R.; Carlson, D.; and Byron, S.: Experiments on Recombination Effects in Rocket Nozzles. AIAA J., vol. 1, no. 2, Feb. 1963, pp. 324-329.

7. Boynton, Frederick P.: Chemical Kinetic Analysis of Rocket Exhaust Temperature Measurements. AIAA J., vol. 2, no. 3, Mar. 1964, pp. 577-578.

8. Kaskan, W. E.: Hydroxyl Concentrations in Rich Hydrogen-Air Flames Held on Porous Burners. Combustion and Flame, vol. 2, no. 3, Sept. 1958, pp. 229-243.

9. Lezberg, Erwin A.; and Lancashire, Richard B.: Recombination of Hydrogen-Air Combustion Products in an Exhaust Nozzle. NASA TN D-1052, 1961.

10. Lezberg, Erwin A.; and Buchele, Donald R.: Some Optical Techniques for Temperature and Concentration Measurements of Combustion in Supersonic Streams. NASA TN D-2441, 1964.

11. Learner, R. C. M.: The Influence of Vibration-Rotation Interaction on Intensities in the Electronic Spectra of Diatomic Molecules. I. The Hydroxyl Radical. Proc. Roy. Soc. (London), ser. A, vol. 269, no. 1338, Sept. 1962, pp. 311-326.

12. Bennett, R. G.; and Dalby, F. W.: Experimental Determination of the Oscillator Strength of the Violet System of OH. J. Chem. Phys., vol. 40, no. 1, Mar. 1, 1964, pp. 1414-1416.

13. Golden, D. M.; Del Greco, F. P.; and Kaufman, F.: Experimental Oscillator Strength of OH, $^2\Sigma^+ \rightarrow {}^2\Pi$, by a Chemical Method. J. Chem. Phys., vol. 39, no. 11, Dec. 1, 1964, pp. 3034-3041.

14. Zeleznik, Frank J., and Gordon, Sanford: A General IBM 704 or 7090 Computer Program for Computation of Chemical Equilibrium Compositions, Rocket Performance, and Chapman-Jouguet Detonations. NASA TN D-1454, 1962.

15. Sarli, V. J.: Investigation of Nonequilibrium Flow Effects in High Expansion Nozzles. NASA CR 52921, Sept. 20, 1963.

16. Zupnik, T. F.; Nilson, E. N.; and Sarli, V. J.: Investigation of Nonequilibrium Flow Effects in High Expansion Ratio Nozzles - Computer Program Manual. NASA CR 54042, Sept. 15, 1964.

17. Westenberg, A. A.; and Favin, S.: Complex Chemical Kinetics in Supersonic Nozzle Flows. Ninth Symposium (International) on Combustion, Academic Press, Inc., 1963, pp. 785-797.

18. Schott, Garry L.: Kinetic Studies of Hydroxyl Radicals in Shock Waves. III: The OH Concentration Maximum in the Hydrogen-Oxygen Reaction. J. Chem. Phys., vol. 32, no. 3, Mar. 1960, pp. 710-716.

19. Fenimore, C. P.; and Jones, G. W.: Radical Recombination and Heat Evolution in H_2-O_2 Flames. Paper Presented at Tenth Symposium (International) on Combustion, Cambridge (England), Aug. 17-21, 1964.

20. Clyne, M. A. A.: Rates of Some Atomic Reactions Involving Hydrogen and Oxygen. Ninth Symposium (International) on Combustion, Academic Press, Inc., 1963, pp. 211-219.

21. Dabora, E. K.: The Influence of a Compressible Boundary on the Propagation of Gaseous Detonations. Rept. No. TR-05170-1-T (AROD-3559-1), Univ. Mich., Dec. 1963.

22. Mitchell, A. C. G.; and Zemansky, M. W.: Resonance Radiation and Excited Atoms. Cambridge Univ. Press, 1961.

23. Penner, S. S.: Quantitative Molecular Spectroscopy and Gas Emissivities. Addison-Wesley Pub. Co., Inc., 1959.

24. Schott, Garry L.; and Bird, Paul F.: Kinetic Studies of Hydroxyl Radicals in Shock Waves. IV - Recombination Rates in Rich Hydrogen-Oxygen Mixtures. J. Chem. Phys., vol. 41, no. 9, Nov. 1, 1964, pp. 2869-2876.

25. Carrington, Tucker: Line Shape and f Value in the $OH\,^2\Sigma^+ - {}^2\Pi$ Transition. J. Chem. Phys., vol. 31, no. 5, Nov. 1959, pp. 1243-1252.

26. Kaskan, Walter E.: Abnormal Excitation of OH in $H_2/O_2/N_2$ Flames. J. Chem. Phys., vol. 31, no. 4, Oct. 1959, pp. 944-956.

27. Momtchiloff, I. N.; Taback, E. D.; and Buswell, R. F.: Kinetics in Hydrogen-Air Flow Systems. I - Calculation of Ignition Delays for Hypersonic Ramjets. Ninth Symposium (International) on Combustion, Academic Press, Inc., 1963, pp. 220-230.